



In silico studies to understand the adsorbent properties of CuO nano-clusters for toxic water soluble dyes

Suneel Kumar Dandabattina, Baswanth Oruganti, Kaleswararao Thaticharla, Anik Sen and Suryakala Duvvuri*

Department of Chemistry, GITAM Institute of Science, GITAM University (Deemed to be), Visakhapatnam-530 045, Andhra Pradesh, India

E-mail: duvurisuryakala@gmail.com

Manuscript received online 01 July 2020, accepted 31 August 2020

Structural analysis of extraordinary efficient CuO-CTAB (cetyl trimethyl ammonium bromide) and CuO-SDS (sodium dodecyl sulphate) nanoparticles and their adsorbing efficiency of significant dyes in aqueous media like Methylene blue, Rhodamine B and Congo red have been calculated using DFT calculations and compared with experimental studies. Structures of the active nano-cluster of $(\text{CuO})_5$, the most stable one derived by DFT methods is the most suitable for the adsorption of such dyes. Optimisations of the three aforementioned dyes have been performed and also the interactions on the CuO cluster have been performed using DFT calculations. A brief charge analysis for the dyes as well as the CuO nano-cluster has been performed, which also indicates the favorable adsorption and the sensor properties of such nano-clusters on different dyes. The quantum chemical descriptions are significant in explaining the adsorption of dyes on the copper(II) oxide at the respective active centers.

Keywords: CuO nano-clusters, density functional theory, partial charges, water soluble dyes, sensor.

Introduction

Dyes are one of the most important ingredients used in large quantities in industries like printing, plastic, pharmaceuticals, textiles, cosmetics, food etc., mostly to colour the products. Dyes such as Methylene blue¹, Rhodamine B², and Congo red³ are commonly used ones. But the industries yield a lot of waste from the uses of such dyes and are generally thrown away. These wastes are mostly toxic and even sometimes carcinogenic and so it should be eliminated before reaching to our water sources of daily use. Purification of such waste in water is a challenging process and also one of the prime goal of our research. There are a lot of processes through which water can be purified like filtration, distillation, osmosis etc. but such dye wastes are very difficult to remove.

Adsorption is one of the mostly used techniques to remove such wastes from the waste water in recent years⁴. Factors like interactions, temperature, pH etc. are very important and mostly influence the adsorption⁵. In our previous, article we discussed that CuO-CTAB nanoparticles acts as a very good adsorbent for the dye Congo red with experi-

mental findings⁶. The explanation of the interactions can be understood still more clearly. The CuO nanoparticles act as the adsorbent and the CTAB as a cationic surfactant which can control the growth rate of various faces of CuO nanoparticles as described in our previous paper⁶. Such adsorbents or additives are also well known to modify the morphology of other particles or crystal structures by adsorbing or interacting at a particular face. The interaction of the additives on a specific plane, reduce the growth of that plane and as a result, other fast growing surfaces disappear and ultimately, the slow growing surface controls the morphology⁷. For the anionic dyes Methylene blue and Rhodamine B, CuO-SDS nanoparticles are used, where CuO nanoparticles acts as the adsorbent and SDS as the anionic surfactant.

The anionic and cationic dyes exhibit respective partial charges, also known as active centers are more favorable for adsorption by any suitable adsorbent¹⁰. This enabled us to calculate the respective partial charges by quantum chemical means and predict the interactions. Even though computational chemistry is not clearly concerned in pollutants elimi-

nation on adsorption from waste water solutions, its wide applications are appreciable in corrosion, super conductors, pharmaceutical chemistry etc.¹¹. Plenty of academic investigations on copper(II) oxide and its catalytic pursuit are well established¹². DFT calculations on such copper(II) oxide clusters or surfaces have been performed aptly in previous literatures^{13–19}.

In this work, we have initially calculated the different structures possible for such CuO nanoparticles which are produced due to the presence of adsorbent as observed in literature^{8,9} by DFT calculations. We have also optimised the different dye structures with quantum chemical calculations. Mulliken charge analysis was performed for the dyes and the CuO nano-cluster to understand the effective interaction sites for the adsorption. Interactions on the specific sites of the most stable (CuO)₅ nano-cluster have been performed for all the three dyes with quantum chemical calculations. The Mulliken charges analysed, provided a proper understanding of the interaction pattern and the binding energies of the dyes on the CuO cluster.

Computational methods:

We have examined different (CuO)_n geometries with n = 1-5 having different spin multiplicities. The low lying singlet, doublet, triplet and quartet spin-states of the clusters are taken in to consideration for calculation. Each balanced (neutral) cluster of copper oxide (CuO)_n is prepared starting with Cu_{n-1}O_{n-1} cluster by adding CuO molecules to the side of Cu_{n-1}O_{n-1} cluster. All the structures are optimized at Becke's three parameter exchange functional with the correlation functional²⁰ of Lee *et al.* (B3LYP)²¹ with CCPVDZ basis set²². Positive harmonic vibrational frequencies confirmed that the optimized structures are minima. The dye molecules are also optimized at the same level of theory. As the dyes binds to nanoclusters through adsorption, the importance of disper-

sion correction is very important for the interactions of the dyes on the copper oxide clusters. Single point calculations with B3LYP-D3 functional was applied with the CCPVDZ basis set to calculate the interaction energies. All calculations have been performed with GAUSSIAN 16²³.

The Mulliken charges have been calculated for all the clusters and the dyes according to the Gaussian 16 formalism. The ionization energy and electron affinity have been calculated for each cluster by performing a single point calculation on removing and adding one electron to the optimized neutral structure. The interaction energies of the dye on the CuO cluster have been calculated using the equation:

$$E_{\text{interaction}} = E_{\text{cluster-dye complex}} - (E_{\text{cluster}} + E_{\text{dye}})$$

The Gibbs free energy have also been calculated for the systems and the interacted species. Single point calculations with SMD solvation model taking water as the solvent were also carried out to verify any solvent effect on the interactions of the dyes with the CuO clusters.

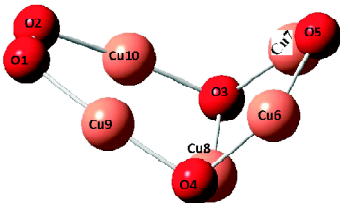
Results and discussion

CuO nanoparticles analysis:

The structures of the (CuO)_n, [n = 1-5] nano-cluster with different possible spin multiplicities are calculated. DFT calculations have already been performed previously and the different stable spin states of the clusters are established at level of theory^{8,9}. In this article, we have similarly calculated the structures possible for the (CuO)_n, [n = 1-5] nano-cluster with different possible spin multiplicities. It was similarly found that the doublet state for Cu₅O₅ is more stable.

No major deviations are observed between the bond distances for the different clusters, but the angle strain for the Cu₅O₅ (doublet) is observed to be the lowest. This makes it to be the most stable structure and also previous reports identified this phenomenon and named it {Cu₅O₅(doublet)}

Table 1. Structure and energy of the doublet spin state of the (CuO)₅ clusters

Cluster	Spin state	Structure	Shape	Energy (Hartree)
Cu ₅ O ₅	Doublet		Boat-shaped non-planar	-8579.2400

Dandabattina *et al.*: In silico studies to understand the adsorbent properties of CuO nano-clusters for toxic water *etc.*

as the “Magic Cluster”⁸.

Furthermore, we have also calculated the electron affinity, ionization energy and relative stabilization energy of the clusters. Electron affinity is defined as the variation in energy of a neutral molecule, when an extra electron is added to it to form the negative ion. In Table 2, we have provided the respective electron affinity of the different clusters, and it has been observed that the highest electron affinity occurs for the cluster (CuO)₅. The definition of the ionization energy is the minimum amount of energy required to remove the most loosely bound electron and it is observed that lowest electron ionization energy occurs for (CuO)₄ and (CuO)₅. The stabilization energy calculated for the clusters as provided for the clusters clearly showed that stabilization energy increases with increase in the cluster size and (CuO)₅ is the most stable one (Table 2).

The band gap of the respective clusters have also been calculated and tabulated in Table 3. The data shows that (CuO)₅ and (CuO)₄ cluster possess the band gap of 1.60 eV and 2.14 eV respectively which is the closest value to the experimentally derived range of 1.20–2.10 eV for CuO nanoparticles. This also proves that such structures of CuO can actively take part in chemical reactions (adsorption). The Mulliken charge analysis of the most stable structure (CuO)₅ is given in Table 4. It showed high negative charge on the

3rd and 4th oxygen atom and high positive charge on the 8th Cu atom ensuring them to be the most important sites for the dye interactions.

Different dye analysis and interaction pattern:

In this article, we have taken 3 different dye molecules: Methylene blue, Rhodamine B and Congo red. Methylene blue, Rhodamine B are cationic dyes and Congo red is anionic dye. The respective structures of the dyes are optimized at B3LYP/CCPVDZ and the Mulliken charges are calculated. We have calculated the salt (solid) form of the respective dyes which is more stable and available in the market and also the cationic and anionic forms of the dyes without the counter ions. Though the salt form is more available in the market but in the aqueous medium, the respective ions will be more easily available to interact with any external moiety. The HOMO, LUMO gaps for all the dyes have been calculated with the counterions. The band gap for both the cationic dyes showed lower values than the band gap of CuO nano-cluster (Table 3 and Table 5) and so both dyes will be very aptly adsorbed on the anionic site i.e. 3rd or 4th oxygen atom of the Cu₅O₅ nano-cluster (Table 1, Table 5). For the anionic dye, Congo red, the calculated band gap is observed to be 2.84 eV, which is way higher than the CuO nano-cluster band gap (Table 3 and Table 5). This indicates lower adsorption of the Congo red dye.

Table 2. Ionization energy, electron affinity, and stabilisation energy for (CuO)_n (n = 1 to 5) cluster

Cluster	Ionization energy (Hartree)	Electron affinity (Hartree)	$\Delta E = E(\text{CuO})_n$ Stabilisation energy (Hartree)
CuO (doublet)	+0.2567	+0.1204	0
Cu ₂ O ₂ (singlet)	+0.2408	+0.1481	-0.1064
Cu ₃ O ₃ (quartet)	+0.2826	+0.1718	-0.2527
Cu ₄ O ₄ (triplet)	+0.2240	+0.1452	-0.3604
Cu ₅ O ₅ (doublet)	+0.2347	+0.1757	-0.5012


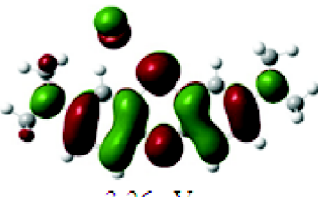
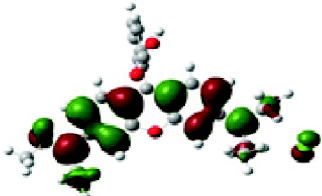
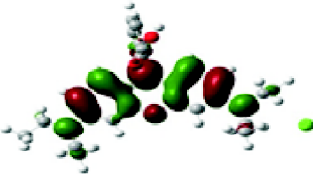

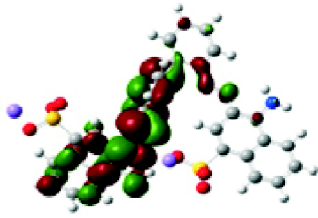
Table 3. HOMO, LUMO energies and the band gap of (CuO)_n, n = 1 to 5 clusters

Cluster	HOMO (Hartree)	LUMO (Hartree)	Band Gap (eV)
CuO	-0.25672	-0.12047	3.71
Cu ₂ O ₂	-0.24089	-0.14848	2.51
Cu ₃ O ₃	-0.28263	0.17180	3.01
Cu ₄ O ₄	-0.22407	-0.14521	2.14
Cu ₅ O ₅	-0.23470	-0.17577	1.60

Table 4. Mulliken charges for Cu₅O₅ cluster

Oxygenatom	Charge on oxygen atom	Copper atom	Charge on copper atom
1	-0.19	6	0.41
2	-0.19	7	0.41
3	-0.58	8	0.63
4	-0.58	9	0.30
5	-0.52	10	0.30

Table 5. The HOMO and LUMO structures and energies of the different dyes along with the band gap (eV)

Dye	HOMO	LUMO	Band gap (H-L) in eV
Methylene blue	 -4.44 eV	 -3.26 eV	1.18
Rhodamine B	 -3.90 eV	 -3.18 eV	0.72
Congo red	 -5.32 eV	 -2.48 eV	2.84

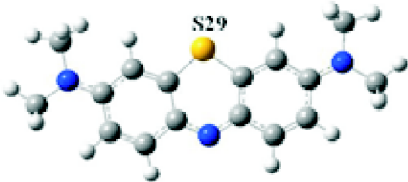
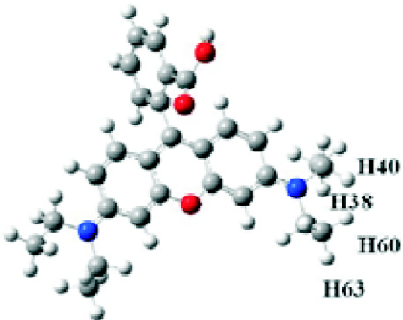
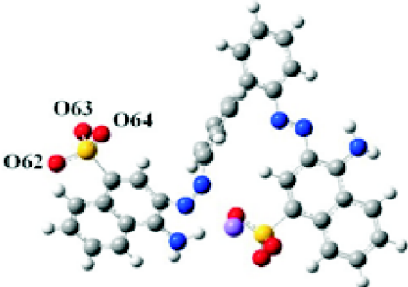
The Mulliken charge analysis for the dyes is performed for both the salt form and the cationic and anionic forms. The salt form showed the higher charge on the counterions, which is not very interesting for the interaction to the cluster. So, the charge analysis for the cationic and anionic forms of the dyes are further analysed for the interactions given in Table 6. The interaction with the $(\text{CuO})_5$ cluster is calculated at this particular sites as given in Table 5. The negative oxygen sites (3rd and 4th oxygen atom of cluster, Table 4) are chosen for interaction of the anionic dye Congo red and the positive site (8th Cu atom of the cluster, Table 4) is chosen for the interactions of the cationic dyes Methylene blue and Rhodamine B.

According to our previous papers^{6,24} on the removal efficiency percentage of all the three different dyes it was observed that at highly acidic pH (pH 2, Fig. 1), Rhodamine B

and Congo red dyes have a removal efficiency percentage of >90%, whereas the removal efficiency of Methylene blue was much lower ~40% (Fig. 1). But with increasing pH the removal efficiency swaps, i.e. higher removal efficiency was observed for Methylene blue and significantly lower for Rhodamine B and Congo red. The rate of downfall of the removal efficiency was observed to be higher for Congo red (Fig. 1).

The interaction pattern and energies of the dyes with the $(\text{CuO})_5$ cluster are given in Table 7. Our theoretical results only showed the interactions and no pH or other effects were taken in considerations. The interactions of the dyes with the CuO cluster directly corroborated with our charge analysis performed in Table 6. Our gas phase and solvent phase results with dispersion corrections showed the same trend which proves that solvation will not have severe effect on

Table 6. Structures and respective selective atoms (Mulliken charges)

	Structures	Atom no.	Mulliken charge
Cationic dye:			
Methylene blue		S29	0.223685
Rhodamine-B		H38, H40, H60, H63	0.039641, 0.038846, 0.037643, 0.038962
Anionic dye:			
Congo red		O62, O63, O64	-0.516819, -0.569675, -0.568673

such results. The anionic dye congo red showed an effect due to salivation is due to the presence of a sodium ion which will have a strong effect on the solvent water, but no change in the trend was observed.

The anionic dye showed the highest interactions as we observed above high charge affinities for the oxygens atoms of the Congo red which interacted the copper ions in the CuO cluster. The cationic dyes Methylene blue and Rhodamine B showed lower interactions than the anionic dyes, due to the lower charges on the interactive atoms of the dyes. Methylene blue showed higher interaction with the CuO cluster than the Rhodamine B as the charge on the sulphur (interacting to the CuO) was higher than the interacting hydrogen atoms of the Methylene blue dye (Table 6).

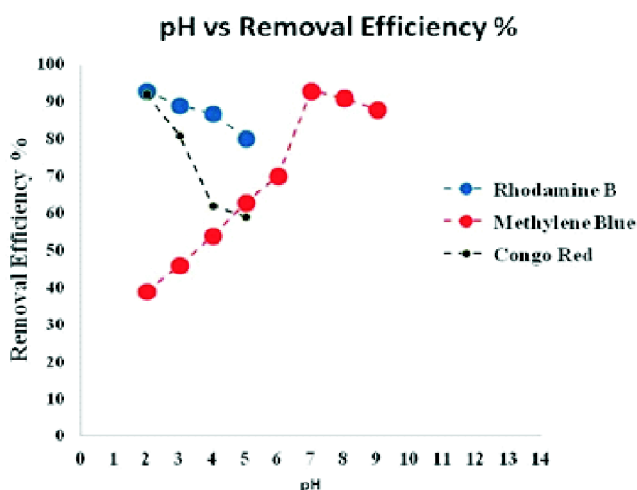


Fig. 1. Plot of pH vs dye removal efficiency of CuO nanoparticles^{6,24}.

Table 7. Interactions of the dyes with $(\text{CuO})_5$ cluster

Bonded dyes	Structure	Interaction energies (kcal/mol)	
		Gas phase	Solvent phase
Methylene blue		-17.9	-19.4
Rhodamine B		-27.4	-22.6
Congo red		-81.3	-31.8

Conclusions

In summary, we have shown a proper description of the dye removal properties of CuO nanoparticles with three different dyes, mostly used in industries. A direct comparison with the experimental results showed a very good justification. Our DFT calculations proved that, (CuO)₅ with doublet spin state is the most stable nano-cluster. The theoretically calculated HOMO-LUMO band gap of (CuO)₅ is in correlation with the experimental band gap of CuO nano-cluster. The DFT calculated partial Mulliken charge analysis of the (CuO)₅ nano-cluster, showed that 8th Cu and 3rd and 4th oxygen atoms are the most significant sites acting as sensor for different toxic water based dyes. The partial Mulliken charge analysis were also performed for the three dyes and based on that, the interactions with the cluster were calculated. The interactions of the dye molecules showed that the binding energies directly corroborated with the charge analysis. Our results showed that the most significant interactions were for the anionic dye Congo red and the interactions of the cationic dyes showed a little less interactions which could be explained from the charge analysis. The solvent analysis showed that there was no change in the trends for the interactions of such dyes which proves that solvation has lower effect on such interactions. Thus the nanoparticles act as a better sensor for particular toxic dye materials and helps to purify the water with such sensor properties. Further work will be performed to understand the interaction pattern of such dyes on the CuO nanoparticles in the presence of surfactants.

Acknowledgements

Authors thank the Department of Science and Technology, India under DST-FIST Program 2013 with Grant No. SR/FST/CSI-252/2013. The authors are thankful to the computational facility of the GITAM (Deemed to be) University, Visakhapatnam, for providing the necessary facilities to complete this work.

References

1. D. L. Postai, C. A. Demarchi, F. Zanatta, D. C. C. Melo and C. A. Rodrigues, *Alexandria Eng. J.*, 2016, **55**, 1713.
2. A. Thakur and H. Kaur, *Inter. J. Indust. Chem.*, 2017, **8**, 175.
3. H. Chen and J. Zhao, *Adsorption*, 2009, **15**, 381.
4. S. Dhananasekaran, R. Palanivel and S. Pappu, *J. Adv. Res.*, 2016, **7**, 113.
5. M. Bansala, D. Singha and V. K. Gargb, *J. Hazard. Mater.*, 2009, **171**, 83.
6. D. Suneel kumar, N. Lalitha Kumari, D. Vasundara, D. Suryakala and K. Ramakrishna, *J. Appl. Chem.*, 2018, **7**, 1428.
7. G. Schmid and D. Fenske, *Phil. Trans. R. Soc. A*, 2010, **368**, 1207.
8. A. Sen and B. Ganguly, *Angew. Chem. Int. Ed.*, 2012, **51**, 11279.
9. G. T. Bae, B. Dellinger and R. W. Hall, *J. Phys. Chem. A*, 2011, **115**, 2087.
10. E. Koblova, A. Ustinov and O. Shcheka, *Appl. Mech. Mater.*, 2015, **709**, 358.
11. D. Bing, T. Li and Y. Jinlong, *J. Chem. Phys.*, 2004, **120**, 2746.
12. L. Armelao, D. Barreca, M. Bertapelle, G. Bottaro, C. Sada and E. Tondello, *Thin Solid Films*, 2003, **442**, 48.
13. M. Abdul Latif, Jenna W. J. Wu, Ryoichi Moriyama, Motoyoshi Nakano, Keijiro Ohshimo and Fuminori Misaizu, *ACS Omega*, 2018, **3**, 18705.
14. B. Shi, S. Weissman, F. Bruneval, L. Kronik and S. Ögüt, *J. Chem. Phys.*, 2018, **149**, 064306.
15. E. Koblova, A. Ustinov, A. Yu and O. Shcheka, *Applied Mechanics and Materials*, 2014, **709**, 358.
16. J. B. Reitz and E. I. Solomon, *J. Am. Chem. Soc.*, 1998, **120**, 11467.
17. J. S. Woertink, P. J. Smeets, M. H. Groothaert, M. A. Vance, B. F. Sels, R. A. Schoonheydt and E. I. Solomon, *PNAS*, 2009, **106**, 18908.
18. D. A. Quist, M. A. Ehudin, A. W. Schaefer, G. L. Schneider, E. I. Solomon and K. D. Karlin, *J. Am. Chem. Soc.*, 2019, **141**, 12682.
19. D. E. Diaz, D. A. Quist, A. E. Herzog, A. W. Schaefer, I. Kipourous, M. Bhadra, E. I. Solomon and K. D. Karlin, *Angew. Chem. Int. Ed.*, 2019, **58**, 17572.
20. A. D. Becke, *Phys. Rev. A*, 1988, **38**, 3098.
21. C. Lee, W. Yang and G. P. Robert, *Phys. Rev. B*, 1988, **37**, 785.
22. J. A. Montgomery, M. J. Frisch, J. W. Ochterski and G. A. Petersson, *J. Chem. Phys.*, 1998, **110**, 2822.
23. M. J. Frisch, G. W. Trucks, H. B. Schlegel, G. E. Scuseria, M. A. Robb, J. R. Cheeseman, G. Scalmani, V. Barone, G. A. Petersson, H. Nakatsuji, X. Li, M. Caricato, A. V. Marenich, J. Bloino, B. G. Janesko, R. Gomperts, B. Mennucci, H. P. Hratchian, J. V. Ortiz, A. F. Izmaylov, J. L. Sonnenberg, D. Williams-Young, F. Ding, F. Lipparini, F. Egidi, J. Goings, B. Peng, A. Petrone, T. Henderson, D. Ranasinghe, V. G. Zakrzewski, J. Gao, N. Rega, G. Zheng, W. Liang, M. Hada, M. Ehara, K. Toyota, R. Fukuda, J.

- Hasegawa, M. Ishida, T. Nakajima, Y. Honda, O. Kitao, H. Nakai, T. Vreven, K. Throssell, J. A. Montgomery (Jr.), J. E. Peralta, F. Ogliaro, M. J. Bearpark, J. J. Heyd, E. N. Brothers, K. N. Kudin, V. N. Staroverov, T. A. Keith, R. Kobayashi, J. Normand, K. Raghavachari, A. P. Rendell, J. C. Burant, S. S. Iyengar, J. Tomasi, M. Cossi, J. M. Millam, M. Klene, C. Adamo, R. Cammi, J. W. Ochterski, R. L. Martin, K. Morokuma, O. Farkas, J. B. Foresman and D. J. Fox, Gaussian, Inc., Wallingford CT, Gaussian 16, Revision A.03, 2016.
24. T. K. Kokkerala, S. K. Dandabattina, L. K. Nethala and S. Duvvuri, *Res. J. Chem. Env.*, 2019, **23**, 68.